Energy, Exergy, and Exergoeconomic (3E) Analysis of Gas Liquefaction and Gas Associated Liquids Recovery Co-Process Based on the Mixed Fluid Cascade Refrigeration Systems

Norouzi, Nima; Bashash Jafarabadi, Zahra; Valizadeh, Ghassem; Hemmati, Mohammad Hossein

Department of Energy Engineering and Physics, Amirkabir University of Technology (Tehran Polytechnic), PO. Box 15875-4413 Tehran, I.R. IRAN

Khajehpour, Hossein*+

Energy Engineering Department, Sharif University of Technology, Tehran, I.R. IRAN

ABSTRACT: *In this study, energy, exergy, and exergoeconomic analysis is performed on the recent trend of joint production of liquefied natural gas and natural gas liquids based on mixed fluid cascade most important of refrigeration systems. The proposed process is first simulated and exergticly analyzed, and finally, an economic model is used to analyze the exergoeconomic performance. The results include the cost of exergy destruction, exergoeconomic factors, and exergy efficiency. The exergy analysis results show that the proposed process's exergy efficiency is about 53.84%, and the destruction rate is 42618 kW with LNG and NGL production rates of 69.00 kg/s and 27.42 kg/s, respectively. Also, results show that the maximum exergoeconomic factor, 69.53%, is related to the second compressor in the liquefaction cycle. The lowest exergoeconomic factor, which is 0.67%, is related to the fourth heat exchanger in the liquefaction cycle. In this process, the distillation tower has the highest relative cost variation (100.81), and the first air cooler in the liquefaction cycle has the smallest relative cost difference (1.08). One of the most costly economic factors is the cost of exergy destruction rates. The second heat exchanger has the exergy destruction cost (768.93 $/GJ), and the first air cooler in the liquefaction cycle has the lowest exergy destruction cost (19.38 $/GJ).*

KEYWORDS: *Exergoeconomic analysis; Gas refinery; Irreversibility; Exergy analysis, optimization.*

INTRoDUCTION

Liquefied Natural Gas (LNG) is one of the most convenient energy carriers, especially for long-distance transportation. This material is produced directly through natural gas and cooling processes. Natural Gas Liquids (NGL), which are used as the main food material in petrochemical processes[1], are also produced by the relevant cooling

** To whom correspondence should be addressed.*
+ E-mail: hkhajehpour2020@gmail.com
1021-9986/2021/4/1391-1410 16/$/6.06

system [2]. LNG operations are classified based on the refrigerant composition and the refrigerant system [1]. Natural gas and LNG liquids are produced in refrigeration processes, of which the refrigeration system is the main part. Increasing the integration level is a key way to improve efficiency and reduce operating and capital costs [3]. In this paper, an integrated alternative process for LNG production and NGL, as proposed, is examined [4]. In particular, exergy analysis is performed to find the proposed process's location, size, and sources of inefficiency. Combining liquefied natural gas leads to less greenhouse gas emissions such as nitrous oxide and sulfur oxide than other fossil fuels and creates less pollution. In addition, liquefied natural gas has significant mass energy of about 50-45 MJ/kg and volumetric energy of about 20-23 MJ/l[1]. Liquefied natural gas is 620 times denser than the gaseous state [2]; this significant volume reduction makes it suitable for storage. Using the pipeline to transport natural gas over distances of more than 3,500 km is not economical, so liquefied natural gas can transport natural gas to remote areas not connected to the pipeline infrastructure [3]. Some of the key issues in small-scale unit liquefaction equipment are 1 (high production cost, 2) profitability and supply chain, 3) system design constraints. Improving the performance of these systems while maintaining their compactness is key to successful development and deployment requirements for small and large units of liquefied natural gas production Efficiency and power consumption are key in all cases. Still, other factors such as equipment, dynamic behavior, and compaction in small-scale units are more important.

Many researchers use experimental methods to evaluate the processes of LNG and natural gas liquefied natural gas. Exergy analysis was performed on four small-scale LNG processes, and the Small modular reactor process was found to have the best energy efficiency of the four processes [4]. A paper [5] performed energy and energy analysis in five conventional LNG operations and concluded that the MFC process's performance is significant in terms of energy consumption quality and quantity. A researcher [6] performed an energy analysis on the industrial refrigeration cycle used in NGL recovery units. The results of the other paper present an exergy analysis of the waterfall cooling cycle used in natural gas liquefaction. The Over-efficiency of successive multi-stage refrigeration cycles was found at 38.5 to indicate the significant potential for improvement[7]. Another simulation performed an energy analysis of the low-temperature refrigeration systems of a multi-stage waterfall used in olivine plants [8]. The stress analysis results show that the main irreversible factors are losses in the pressure system and driving forces in the heat exchangers. Another model proposed a new method for increasing the power of absorption refrigeration machines [9].

However, no term directly covers the costs associated with exergy degradation in exergy analysis, which can only be identified through exergoeconomic analysis. The analysis was performed based on the PRICO liquefaction process, i.e., strange, economic, and exogenous analyzes by researchers performed in [7,8] performed economic and operational analysis on the natural gas separation process. The results showed the highest percentage increase in unit exergoeconomic costs for the density and methane sectors. Exergoeconomic analysis of the industrial refrigeration cycle was investigated in [10], in which the effect of component inefficiency on fuel station consumption, materials, and resulting faults was analyzed and measured. A simulation [11] presented an exergoeconomic analysis of the refrigeration cycle in which the components of the cycle are compared based on initial capital and non-refundable costs. Research [12] conducted an exergoeconomic analysis of a dual-effect absorption refrigeration system with direct combustion of natural gas in which a fixed investment is considered for every subsystem. Another study performed an exergoeconomic analysis of two-ejector and two-ejector collision systems to compare the effect of different operating parameters on the flow rate of investment product costs and total system costs[13].

Natural gas liquefaction processes cost a lot of initial investment and energy consumption. Therefore, improving the performance of deep cooling processes can help reduce energy consumption and investment costs in this area. Therefore, using multi-component refrigerants in liquefaction systems reduces the number of equipment compared to cascading liquefaction systems three and covers a large temperature surface in the heat exchanger, reducing power consumption researchers considered. On the other hand, determining the optimal composition and size of the heat exchanger can reduce operating costs and project investment. A reference [4] stated that the main goal designing a liquefied gas production unit is to operate by minimizing energy consumption and maximizing liquefied natural gas production when product demand rates change and under different ambient temperature conditions. A study [5] proposed an optimal control structure for the two-stage multi-component refrigeration process to maintain the compressor power consumption in optimal conditions. A researcher and his colleagues [6] performed a sensitivity analysis on natural gas liquefaction cycles using peaks concerning changes in environmental and operational conditions (such as changes in flow rate, pressure, temperature, and percentage of feed gas and refrigerant components). They concluded that the multi-component refrigerant cycle consumes less power than the expander cycle and is, in most cases, more sensitive to environmental and operational changes. Some researchers [7] examined a class from a thermodynamic and economic point of view with four different objective functions and concluded that the greatest reduction in investment cost in compressors and heat exchangers is achieved when the objective function is to reduce the overall heat transfer coefficient and power consumption simultaneously. Another study [8] compared the multi-component refrigerant process with propane pre-cooler to the two-stage multi-component refrigerant process concerning liquefied natural gas and LPG production. It concluded that the two-stage multi-component refrigerant process has 15% more capacity than the multi-component refrigerant process with a propane pre-cooler.

A work [9] optimized the multi-component refrigerant natural gas liquefaction cycle with three different pre-coolers, including absorption pre-coolers, multi-component refrigerants, and propane. Multi-component with propane pre-cooler is 12.6% and 18.4% more than the absorption pre-cooler cycle, respectively. Other researchers [10] reported the optimal operating conditions for the liquefaction process of a two-stage multi-component refrigerant concerning the power required to use the production, storage, and discharge of the vessel as a target, and to calculate the optimal values of design variables They used the combined optimization method of sequential square algorithm and genetic algorithm. The results showed that the power consumption was reduced by 34.5% by obtaining the optimal operating conditions compared to the reference results. A study [11] stated that the power consumption of compressors depends on the environmental conditions so that the cold environment helps the refrigeration and, in turn, reduces the specific compression energy. Another literature reference [12] examined four processes suitable for the use of floating production, storage, and discharge, including the one- and two-stage multi-component refrigerant process, the Nietzsche liquefaction process, and the two-stage nitrogen expansion, and showed that the multi-component refrigerant process Two-layer requires less refrigerant consumption and discharge than other processes and has more production capacity. Another research [13] applied exergy-based methods (environmental and economic exergy) to the Perico process, a multi-component, single-layer refrigerant process because the heat exchanger has the most exergy loss and costs. Related to this, they suggest improving the performance of this section. Some researchers [14] investigated the effect of leakage on the two-component multi-component refrigerant process and used an innovative method to analyze leakage at two high-pressure points of the system. Their results show that leakage will slightly reduce specific labor consumption and significantly reduce liquefied natural gas production. Also, leakage reduces the risk of temperature interference in heat exchangers due to reducing the temperature difference between Increases in hot and cold currents.

In this paper, exergy analysis and exergoeconomic analysis are used for alternative processes of recent simultaneous LNG and NGL with appropriate energy consumption and high ethane recovery. After identifying high consumption and inefficient items, a relationship between economic costs and investment is introduced, and components with higher exergy destruction costs are identified. These results help policymakers and technicians to improve the process by optimizing the less efficient cycles and utilities. Briefly, this paper aims to analyze an LNG and NGL coproduction plant energetic and exergoeconomicly to detect its leakages and improve the cycle by replacing and filling the leakages and gaps.

EXPERIMENTAL SECTION

Fig. 1 The Process Flow Diagram (PFD) of the MFC is shown. As we have seen, the recovery of natural gas liquids and LNG production is done in an integrated process (*Mehrpooya et al.*, 2014). A brief description is provided, and for more details, you can refer to the available reference.

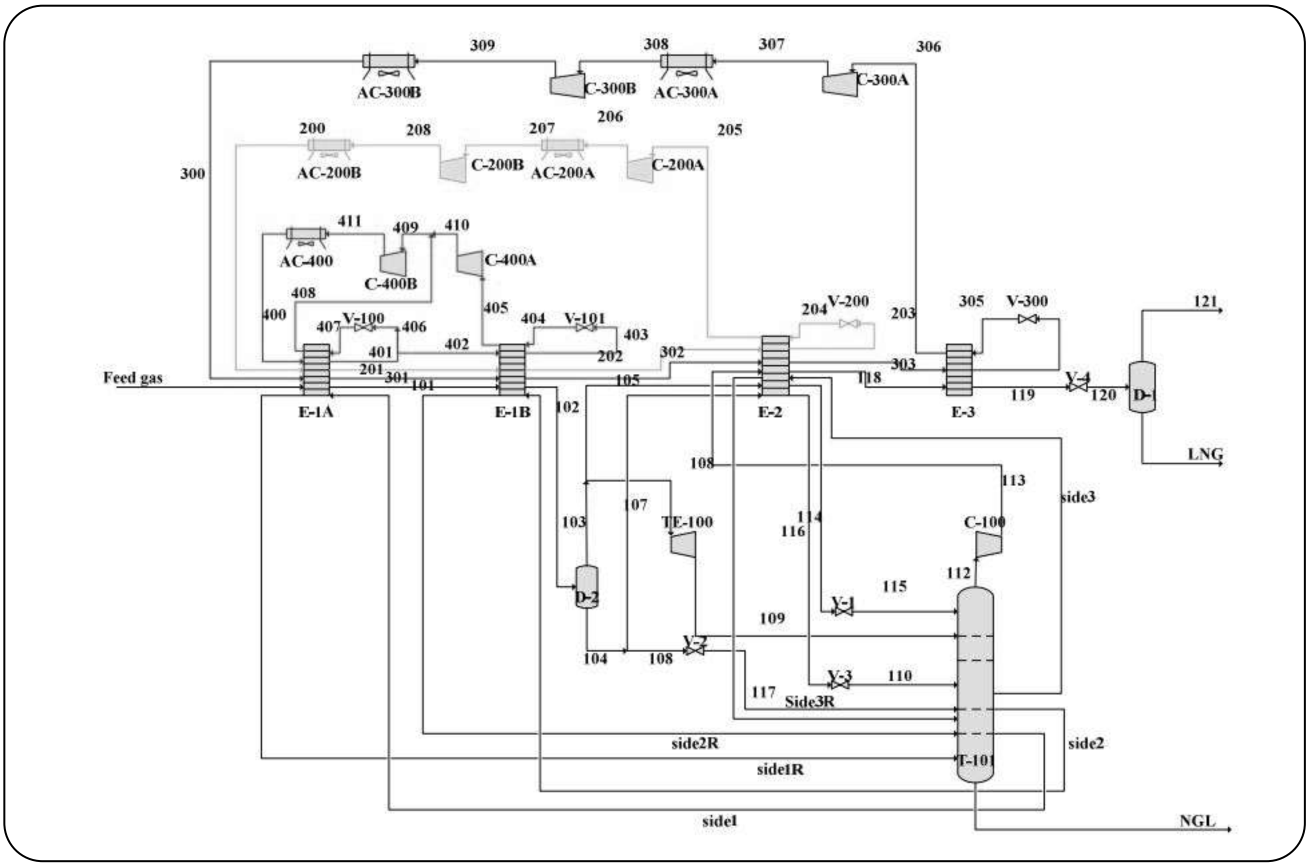

Fig. 1: Process flow diagram for MFC formation[1,2].

NGL Recovery Section

The purified and pre-refined natural gas feed, with the compound shown in Table 1, enters the plant at 37 °C and 63.09 bar and is cooled in two stages: in the E-1A heat exchanger up to 3 °C., then in the heat exchanger to -30 °C the second case, E-1B. 40% of the D-2 gas product is directed to the E-2 converter and cooled to about -88 °C (current 114). Next, current 114 is routed through the J-T valve as a return tower to the top of the de-methane tower. A turbine expander expands another portion of the exhaust steam from the D-2 just below the tower's top before it enters the methane cleaner. Also, the lower part of the liquid is poured into two parts: stream 108 enters the column to be fragmented through the JT valve passage, the other part of stream 107 is cooled through E-2 to -30 °C through the JT valve enters the tower. The Demethanizer tower operates on about 25 bars and includes standard trays used in methanizer destroyer columns. The tower consists of three liquid receiving trays to provide the heat needed to separate the volatile components from the natural gas liquids produced. The required heat is supplied by two multi-flow heat exchangers E-1A and E-1B. Side currents 1, 2, and 3 enter the heat exchanger at 17.7, -7.7, and -54 °C and return to the tower at 35, 0, and -15 °C, respectively. This configuration required no boiler, and ethane extraction increased to 92% [15, 16].

Liquefaction section

A thin stream of gas exits the methane tower at about -97 °C, and 25 rods enter the LNG section. Current 112 is compressed about 63 times in the C-100 compressor and then cooled to about -85.25 °C in the E-2. In this process, the final cooling in LNG production occurs in the E-3 heat exchanger, and the current 119 is cooled to about -162.5 °C and delivered to the D-1 flash cylinder by passing through the J-T valve. The liquid D-1 is at atmospheric pressure LNG [16-22].

Cooling system

The advantages of mixed cooling systems, including high thermal efficiency and high flexibility, have been used in the proposed integrated process [23].

Table 1: MFC configuration main streams data.

		Feed gas	Cycle 200	Cycle 300	Cycle 400	NGL	LNG
Composition	methane	82.17	10.65	39.6	0	0.67	97.83
	ethane	6.65	37.4	0	0	47.35	0.62
	propane	5.13	19.64	0	73	39.18	0.06
	n-butane	0	0	0	15	0	0
	ethylene	0	31.3	41.58	11	0	0
	nitrogen	0.5	0	17.82	0	0	0.41
	Carbon Dioxide	0.2	0	0	0	1.07	0.07
	C^{4+}	4.36	0	0	0	10.72	0
Operation Condition	Temperature (°C)	36.63	34.65	34.65	39.6	28.12	-161.11
	Pressure (bar)	62.46	27.62	28.71	16.73	24.75	1
	molar flow (kmol/hr)	17820	18810	12375	27126	2379.96	15161.85

Hottest cycle (cycle 400)

The process flow diagram for this cycle is shown in red lines in Fig.1. It is also a heating tank for 200 and 300 refrigeration cycles. The 400 refrigeration cycle is a mixture of propane and ethane. Refrigerants are shown in Table 1[24].

Intermediate cycle (cycle 200)

This cycle, shown by the green lines in Fig. 1, provides part of the cooling required for the liquefaction section and most of the NGL recovery unit's cooling. The middle cycle is also a heat reservoir for the coldest cycle, cycle 300. The coolers in this cycle are methane, ethane, propane, and ethylene[25].

Liquidation cycle (cycle 300)

This cycle's main function, shown by the blue lines Fig. 1, provides the cooling required for liquefaction and sub-cooling. The coolant in this cycle is methane, ethylene, and nitrogen. The thermodynamic data of the flows are shown in Table 2[26].

Operation simulation

The integrated process simulation provided by the Aspen HYSYS program is performed using the Peng-Robinson-Stryjek-Vera case (PRSV) equation. The equipment's main power consumption in this process, Specific Energy Consumption (SEC), and performance parameter (COP) are shown in Table 3[27].

Exergy analysis

Exergy is a term for thermodynamics and refers to the maximum useful force received from a system to achieve thermodynamic exchange. Simple but unscientific definition: Exergy is the total energy consumed, for example, to keep the car steady. The wasted part of the energy is called energy [28-33]. In thermodynamics, the system's exergy is the most useful work possible in a process that balances the system with the heat source. When the environment is around the spring, exergy is the system's potential for change when it reaches equilibrium with the environment. Exergy is the energy available for use. Once the system and the environment are in equilibrium, the exergy becomes zero. The study of exergy was also the first goal of thermodynamics. The term exergy was coined in 1956 by Zoran Rent using the Greek words ex and ergon [34]. Energy is never lost in a process but changes from one form to another.

Conversely, exergy is an irreversible factor in a process due to increased entropy. Exergy always disappears when there is a temperature change. This destruction is proportional to the increase in entropy of the system with its surroundings [35].

Destroyed exergy is called anergy. For an isothermal process, exergy and energy are interchangeable. Exergy analysis is performed in the field of the industrial environment for more efficient use of energy. Engineers use exergy analysis to optimize applications with physical constraints, such as choosing the best use of roof space

Table 2: The thermodynamical exergy model of this system [13, 14].

	Description	Equation
1	Exergy balance	$Ex_Q + \sum m_i ex_i = \sum m_e ex_e + Ex_w + Ex_D$
2	Exergy equation	$ex = ex_{ph} + ex_{ch}$
3	Physical exergy	$ex_{ph} = (h_2 - h_1) + T_0 (s_2 - s_1)$
4	Chemical exergy	$ex_{mix}^{ch} = \sum X_i ex^{ch} + RT_0 \sum \ln X_i$
5	Exergy Efficiency	$e = \frac{Ex_p}{Ex_F}$

for solar energy technology. Ecologists and design engineers often consider a spring reference mode that may differ from the actual system environment [36]. Energy is a combination of the system and its environment because it depends on both the system and the environment. The exergy of the system is in equilibrium with zero environments. Exergy is neither the thermodynamic property of matter nor the thermodynamic potential of the system. Exergy and energy both have units of joules. The internal energy is always measured from a fixed reference state and is, therefore, a state function. Some authorities define system exergy as a variable with environmental changes, not a state's function.

Some other authors offer a slightly different definition in which they define the environment around the absolute, immutable reference state, replacing the system state's property alone. Exergy applications when the first law of thermodynamics is expressed as the principle of energy conservation, we are dealing with a number of different forms of energy [37]. From an engineering point of view, a quantity of energy has quality. In general, quality means the degree of usefulness. Reactions of work and heat cause changes in systems. Previous observations show that work is much more important than the reaction of heat to change the system's state. Since work reactions have a high degree of usefulness, it is said that they have a higher quality than heat reactions. Even the second law of thermodynamics sets a higher standard for work than heat. Work is completely converted to heat, but heat conversion to work by a thermodynamic cycle device is very limited. Therefore, work is more useful than heat, and it is sometimes very difficult to obtain. Exergy is one way of energy analysis, including all the energies of the fluid flow. This energy can be due to the movement of the reaction or anything else. G = H-TS is the basis of exergy analysis[4-10].

The above equation should be used instead of the energy balance, for example, for a current in a reactor. In recent decades, process integration issues have been raised. Previously, it was thought that only by using the single processes of a system can the system's best-operating conditions be achieved, but the study of the interaction of processes and their impact on each other leads to the whole system's efficiency. This method has two parts: the analytical tool Exergy and the applied tool pinch. Exergy is based on thermodynamics' second law, and pinch is based on thermodynamics' first law [11]. The exergy method is a solution for thermodynamic analysis of processes, defined as a universal measure of the working potential or quality of various forms of energy concerning an environment. An exergy balance application expresses how the process consumes much of the usable work potential entered into the process. This amount of loss is the same as irreversibility (see Table 2).

Exergy is defined as the maximum useful theoretical work (axial work or electrical work) when the system reaches environmental conditions through a process of its specific thermodynamic state [27]. Unlike energy, exergy is not preserved and is lost due to irreversible phenomena in real processes (e.g., heat transfer, friction, pressure drop in the valve). Exergy analysis allows many shortcomings of energy analysis to be remedied. Exergy analysis is based on the second law of thermodynamics and is useful in identifying the causes, location, and values of process inefficiencies and helps to improve systems. By ignoring the kinetic energy and the potential of the working fluid, the exergy of the current in the steady state is expressed as Eq. (3) [22].

Where h_i and s_i represent the enthalpy and entropy of the working fluid, respectively, and h_0 and s_0 represent the enthalpy and entropy of the working fluid at ambient temperature; respectively, T_0 is also the ambient temperature.

Table 3: Exergoeconomic formulations[38, 39].

	Exergoeconomics	
7	Exergy stream cost rate	$\dot{C}_j = c_j \times \dot{E}_j$
8	Component cost balance	$\sum C_{j,k,in} + Z_k = \sum C_{j,k,out}$
9	Component-related cost rate	$\dot{Z}_k = Z_k^{CL} + Z_k^{OM}$
10	The component relative cost difference	$r_k = \frac{C_{p,k} - C_{F,k}}{C_{F,k}}$
11	Component exergoeconomic factor	$f_k = \frac{Z_k}{Z_k + C_{D,k}}$

Exergy loss in the refrigeration cycle components, compressor, condenser and throttle valve, heat exchanger, and fuzzy separator is given in equation (1) [22-33]. e_{in} and e_{out} are the exergy of entry and exit, respectively. The exergy efficiency (competence coefficient) of the whole natural gas liquefaction system can be calculated from equation (13).

$$e = \frac{Ex_{LNG+NGL}}{Ex_{NG} + Ex_{energy\ demand}} \quad (6)$$

$Ex_{LNG+NGL}$ exergy of LNG and NGL products and Ex_{NG} exergy gas flow input feed.

Exergoeconomic

The method for exergoeconomic analysis is similar to an exergoenvironmental analysis. It combines an exergy analysis of the energy conversion system with an economic analysis based on the Total Revenue Requirements (TRR) method, covering the energy conversion system's entire life cycle. Initially, the total capital investment is calculated. The total annual revenue needed is calculated based on economic, financial, operational, and market input parameters. This TRR represents the cost of producing system products and offsets all costs incurred each year of the project's economic life to guarantee an industrial plant. After that, the product's annual variable costs related to investment, operation, maintenance, fueling, and other costs (cost categories) are leveled. This equipment is converted into a series of fixed payments equivalent to the annuity. Next, by calculating each material and energy flow's specific cost rate, the costs are assigned to the respective exergy flows. Since the exergoeconomic analysis is well established, only the analogy formulas with those used for environmental analysis are presented in Table 3.

RESULTS AND DISCUSSION

In an exergy analysis, the maximum useful performance achieved is calculated with a certain amount of energy. Important parameters obtained from exergy analysis are exergy degradation, exergy efficiency, and exergy degradation ratio, as shown by the following expression [38-42]:

$$E'_D = E'_F - E_P \quad (12)$$

$$\varepsilon = \frac{E'_P}{E'_F} \quad or \quad \varepsilon = 1 - \frac{E'_D}{E'_F} \quad (13)$$

$$y'_D = \frac{E'_{D,k}}{E'_{F,tot}} \quad (14)$$

E indicates the degree of exergy, while the codes F, P, D, and k indicate fuel, product, degradation, and component, respectively. Also, exergy data for currents are shown in Table 5.

Exergoeconomic provides information for system design that is not possible through conventional energy analysis and economic evaluation by analyzing energy and economic principles. In energy systems, economic analysis and improvement, annual investment, fuel cost, and system maintenance cost must be calculated. In this paper, the Total Revenue Requirement (TRR) method, as developed by the Electricity Research Institute [34-57], is used to analyze the system economically (see Table 6).

Table 4: Thermodynamic data for MFC configuration material streams.

Stream no.	Temperature(°C)	Pressure (bar)	Flow (kmol/h)	Stream no.	Temperature (°C)	Pressure (bar)	Flow (kmol/hr.)
feed	36.63	62.46	17820	300	34.65	28.71	12375
101	2.97	62.46	17820	301	2.97	28.71	12375
102	-29.7	62.46	17820	302	-26.73	28.71	12375
103	-29.7	62.46	16384.5	303	-84.35	28.71	12375
104	-29.7	62.46	1434.51	304	-157.41	28.71	12375
105	-29.7	62.46	6553.8	305	-165.18	3.47	12375
106	-29.7	62.46	9830.7	306	-88.66	3.47	12375
107	-29.7	62.46	430.65	307	53.16	24.75	12375
108	-29.7	62.46	1004.85	308	34.65	24.75	12375
109	-64.48	25.74	9830.7	309	48.02	28.71	12375
110	-62.23	24.75	430.65	400	39.6	16.73	27126
112	-95.98	24.75	15439.05	401	8.71	16.73	27126
113	-36.35	62.37	15439.05	402	8.71	16.73	10800.9
114	-87.12	62.46	6553.8	403	-21.78	16.73	10800.9
115	-96.41	24.75	6553.8	404	-29.09	2.97	10800.9
116	-49.5	62.46	430.65	405	1.24	2.97	10800.9
117	-47.4	25.25	1004.85	406	8.71	16.73	16325.1
118	-84.35	62.37	15439.05	407	-0.34	6.63	16325.1
119	-160.88	62.37	15439.05	408	33.24	6.63	16325.1
120	-161.11	1	15439.05	409	34.99	6.63	27126
121	-161.11	1	277.2	410	37.61	6.63	10800.9
200	34.65	27.62	18810	411	81.04	16.73	27126
201	2.97	27.62	18810	side1	17.56	24.75	2277
202	-26.73	27.62	18810	side2	-7.8	24.75	2277
203	-80.69	27.62	18810	side3	-53.54	24.75	2277
204	-90.08	3.07	18810	side1R	34.65	24.75	2277
205	-29.42	3.07	18810	side2R	0	24.75	2277
206	66.95	14.85	18810	side3R	-14.85	24.75	2277
207	34.65	14.85	18810	NGL	28.12	24.75	2379.96
208	77.12	27.62	18810	LNG	-161.11	1	15161.85

Table 5: Main equipment power consumption, specific energy consumption, and coefficient of performance.

	Component Name	Power(kW)*
Compressors	C-100	6064.86
	C-200A	24107.69
	C-200B	10203.72
	C-300A	16807.21
	C-300B	1664.71
	C-400A	7123.01
	C-400B	21791.78
Turbo expander	TE-100	2319.30
Air coolers	AC-200A	92.60
	AC-200B	1393.89
	AC-300A	299.75
	AC-300B	232.81
	AC-400	4851.01
Specific energy (kWh/kg LNG)		0.36
COP		2.22
Mechanical efficiency		0.75

In this method, all costs, including return on investment, are calculated. Based on the assumptions of table 7, equipment and fuel prices and total annual revenue are calculated. Finally, all costs, including maintenance and fuel costs, are balanced during system operation. As the years of system operation increase, investment costs decrease, while fuel costs increase. Therefore, the amount of the required total annual income balance (TRRL) is calculated by the return on investment factor (CRF) and monetary depreciation given in Eq. (15) [57-97]:

$$TRR_L = CRF\sum_{1}^{BL}\frac{TRR_j}{(1+i_{eff})^j} \tag{15}$$

TRRj represents the total revenue required in the fourth year of system operation, and BL represents the system's economic life cycle as measured in years. i_{eff} is the average annual rate of effective depreciation. The return on equity (CRF) is calculated as follows:

$$CRF = \frac{i_{eff}(1+i_{eff})^{BL}}{(1+i_{eff})^{BL}-1} \tag{16}$$

In this study, the TRRj is the sum of four annual values, including the minimum return on investment (ROI), the total return on investment (TCR), operating and maintenance costs (OMC), and fuel costs (FC).

The equations for estimating the equipment's cost are illustrated in Table 8 and the results calculated are illustrated in Table 9.

There is more than one unknown variable for some types of equipment with more than one output flux, so the auxiliary equations are determined according to P and F [19, 97-103] for these types of equipment. Tables 8 and 9 show the cost balance and auxiliary model of a system, respectively. Given that for some components, the equations are not solved independently, a set of linear-dependent equations must be solved simultaneously. A computer program has been developed in MATLAB to solve the cost equilibrium and auxiliary equations to obtain the unit surplus cost per stream, as shown in Table 9.

This paper applies external energy and catastrophic economics analysis for modern integrated alternative operations for the simultaneous production of LNG and LNG. Exergy analysis The results of this process are shown in Table 10. In this process, the highest irreversible degree

Table 6: Exergy and unit exergy cost for each stream of MFC configuration.

Stream no.	$\dot{E}^{PH}$ (kW)	$\dot{E}^{CH}$ (kW)	$\dot{E}^{TOT}$ (kW)	C ($/GJ)	Stream no.	$\dot{E}^{PH}$ (kW)	$\dot{E}^{CH}$ (kW)	$\dot{E}^{TOT}$ (kW)	C ($/GJ)
feed	48348.63	4898446.74	4946795.37	19.54	300	27854.64	3114836.01	3142691.64	74.64
101	48528.81	4898446.74	4946975.55	19.55	301	27956.61	3114836.01	3142792.62	74.65
102	50389.02	4898446.74	4948834.77	19.59	302	28605.06	3114836.01	3143441.07	74.66
103	46268.64	4220135.37	4266404.01	19.59	303	39361.41	3114836.01	3154197.42	74.69
104	3563.01	678867.75	682430.76	19.59	304	58791.15	3114836.01	3173627.16	74.72
105	18507.06	1688053.95	1706562	19.59	305	57488.31	3114836.01	3172325.31	74.75
106	27760.59	2532081.42	2559842.01	19.59	306	14192.64	3114836.01	3129028.65	74.75
107	1069.2	203659.83	204729.03	19.59	307	26860.68	3114836.01	3141696.69	74.64
108	2493.81	475207.92	477701.73	19.59	308	26696.34	3114836.01	3141532.35	74.64
109	24358.95	2532081.42	2556440.37	19.59	309	27960.57	3114836.01	3142796.58	74.64
110	1072.17	203660.82	204732.99	19.62	400	40391.01	16367272.02	16407663.03	104.35
112	40038.57	3584843.46	3624882.03	19.68	401	40113.81	16367272.02	16407385.83	104.35
113	44125.29	3584843.46	3628968.75	19.72	402	15972.66	6517041.3	6533013.96	104.35
114	23491.71	1688053.95	1711545.66	19.78	403	17192.34	6517041.3	6534233.64	104.35
115	22882.86	1688053.95	1710936.81	19.79	404	16748.82	6517041.3	6533790.12	104.36
116	1128.6	203659.83	204788.43	19.61	405	8046.72	6517041.3	6525089.01	104.36
117	2322.54	475207.92	477530.46	19.6	406	24141.15	9850230.72	9874371.87	104.35
118	54381.69	3584843.46	3639225.15	19.9	407	23611.5	9850230.72	9873842.22	104.35
119	75832.02	3584843.46	3660676.47	20.25	408	20181.15	9850230.72	9870411.87	104.35
120	73449.09	3584843.46	3658293.54	20.26	409	33565.95	16367272.02	16400837.97	104.34
121	278.19	58138.74	58415.94	20.26	410	13389.75	6517041.3	6530431.05	104.31
200	39962.34	7923313.53	7963275.87	77.43	411	50562.27	16367272.02	16417834.29	104.27
201	41451.3	7923313.53	7964764.83	77.47	side1	4264.92	1172245.14	1176510.06	104.35
202	45980.55	7923313.53	7969294.08	77.49	side2	4636.17	1122250.14	1126887.3	104.36
203	54480.69	7923313.53	7977794.22	77.5	side3	5804.37	1021246.38	1027050.75	104.36
204	53015.49	7923313.53	7976329.02	77.51	side1R	4287.69	1172179.8	1176468.48	104.35
205	15757.83	7923313.53	7939071.36	77.51	side2R	4541.13	1121920.47	1126461.6	104.36
206	34254	7923313.53	7957567.53	77.44	side3R	4920.3	1021176.09	1026096.39	104.36
207	33429.33	7923313.53	7956743.85	77.45	NGL	4116.42	1317520.71	1321637.13	19.88
208	41364.18	7923313.53	7964677.71	77.41	LNG	73131.3	3526745.31	3599876.61	20.46

Table 7: Economic constants and assumptions.

Economic parameters	Value
The average annual rate of the cost of money (i_{eff})	10%
Average nominal inflation rate for the operating and maintenance cost (r_{OMC})	5%
Average nominal inflation rate for fuel (r_{FC})	5%
Plant economic life (life spawn)	25 years
Total annual operating hours of the system operation at full load	7300

Table 8: Thermoeconomic cost model.

Equipment	Purchased equipment cost functions
Compressor	$C_C = 7.90(HP)^{0.62}$ C_C= Cost of Compressor (k$)
Heat exchanger	$C = 1.218 f_d f_m f_p C_b$ $C_b = \exp[8.821 - 0.30863(\ln A) + 0.0681(\ln A)^2]$, 150<A<12000, $f_d = \exp(-1.1156 + 0.0906 \ln A)$, f_M= Material Factor, f_P=Pressure factor
Separator	$C = 1.218[a + bW]$, K$ 5<W a= 42, b=1.63
Air cooler	$C_{AC} = 1.218 f_m f_P \exp[a + b \ln Q + c(\ln Q)^2]$, Q in KSCFM C_{AC}= Cost of Air cooler (k$) f_m=Material Factor, f_P=Pressure Factor, a=0.4692, b=0.1203, c=0.0931
Turbo Expander	$C_{TE} = 0.378(HP)^{0.81}$ C_{TE}= Cost of Turbo Expander (k$)
Absorption	$C_T = 1.218[f_1 C_b + N f_2 f_3 f_4 C_t + C_{p1}]$ $C_t = 457.7 \exp(0.1739D)$, 2<D $C_b = 1.218 \exp[6.629 + 0.1826(\ln W) + 0.02297(\ln W)^2]$, 4250<W<980,000 lb shell $C_{p1} = 300D^{0.7396}L^{0.7068}$, 3<D<21, 27<L f_1= Material Factor, $f_2 = 1.189 + 0.0577D$, f_3=Tray Types Factor, $f4 = \frac{2.25}{(1.0414)^N}$

Table 9: Equipment and investment costs for MFC process components.

	PEC ($)	$\dot{Z}^{CI}$ ($/hr)	$\dot{Z}^{OM}$ ($/hr)	$\dot{Z}$ ($/hr)
E-1A	121939.65	7.93	0.20	8.13
E-1B	79044.63	5.14	0.13	5.27
E-2	126424.61	8.22	0.21	8.42
E-3	65199.1	4.24	0.11	4.35
AC-200A	56207.1	3.65	0.09	3.74
AC-200B	56207.1	3.65	0.09	3.74
AC-300A	24571.61	1.59	0.04	1.63
AC-300B	56207.1	3.65	0.09	3.74
AC-400	102692.22	6.67	0.17	6.84
C-100	2077897.18	135.08	3.43	138.50
C-200A	4888871.94	317.80	8.06	325.86
C-200B	2868815.24	186.49	4.73	191.22
C-300A	3909123.36	254.11	6.44	260.56
C-300B	932187.65	60.60	1.53	62.13
C-400A	2295746.13	149.23	3.78	153.01
C-400B	4607461.63	299.50	7.59	307.10
TE-100	252500.89	16.41	0.42	16.83
D-1	54833.28	3.56	0.09	3.65
D-2	74233.24	4.82	0.12	4.94
T-101	77069.99	5.01	0.13	5.14

Table 10: Exergy analysis of MFC process.

Component	$\dot{E}_D$ (kW)	ε (%)	Component	$\dot{E}_D$ (kW)	ε (%)
C-100	1917.7389	67.3794	T-101	1699.4142	49.5099
C-200A	5368.9086	76.725	E-1A	1915.1154	96.7923
C-200B	2166.9912	77.7645	E-1B	1423.9863	96.7527
C-300A	3970.7019	75.3786	E-2	2700.6903	95.8716
C-300B	383.5854	75.9528	E-3	2414.9268	93.3669
C-400A	1709.3142	75.0024	V-1	609.0975	53.46
C-400B	4577.6412	77.9922	V-2	171.0324	52.47
TE-100	1106.1072	66.8151	V-3	55.5984	68.31
AC-200A	686.9115	97.02	V-4	2382.9102	30.69
AC-200B	826.8381	97.02	V-100	529.3035	29.7
AC-300A	269.9235	98.01	V-101	443.0349	39.6
AC-300B	280.8531	98.01	V-200	1465.5465	89.1
AC-400	1807.7301	95.04	V-300	1302.6915	85.14
MIX-1	4.7223	99.98			

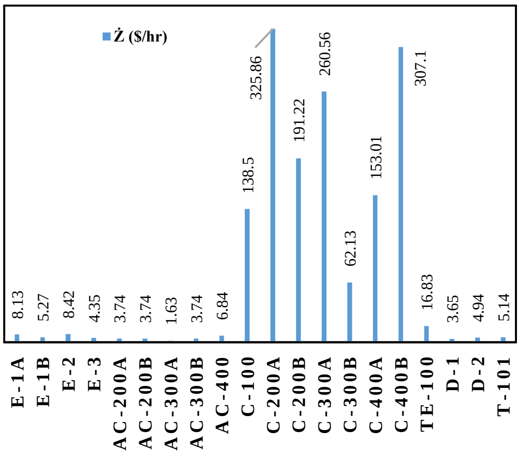

Fig. 2: The total thermoeconomic cost of each component

is related to the C-200A compressor with a value of 5422 kW, and the second-highest value is related to the C-400B, C-300A, and E-2 units. The exergy efficiency of expansion valves was lower than in other units. This process's external energy efficiency is about 53.82%, and the total output energy degradation is equal to 42617.4 kW (Figs. 3 and 4).

Through exergoeconomic analysis, a rational relationship can be established between the initial investment and current costs due to failure, which enables us to determine whether the system works economically or not. In this method, first, the investment costs, as shown in Table 9, are estimated, and then using the method of total revenue requirement and writing the cost balance equation, the unit cost of exergy for each flow is determined (Table 6). Finally, the exergoeconomic factor and the relative cost difference are determined through exergoeconomic analysis, and the results are shown in Table 11. The amount of exergoeconomic factors represents information about the cost of investment and over-efficiency of the system: Large values indicate that to reduce system costs, system costs must be reduced. Elements, while small values indicate that system performance and efficiency should be improved to reduce system cost.

This process shows that the C-300B compressor has the highest economic coefficient (69.52), and the lowest economic factor is connected to the tower (4.70). The relative cost difference indicates the relative increase in the fuel's exergy cost in a material, which is important in evaluating and improving the system. In this process, the T-101 de-methanizer tower has the highest relative cost difference (66.75), and the AC-300A air conditioner has the lowest relative cost difference (50.39). Exergy cost values for fuel and products determine the cost of exergy rates in a commodity. The maximum fuel rate is

Table 11: Rresults of exergoeconomic study of MFC process.

Component	$\dot{E}_D$ (kW)	C_F (\$/GJ)	C_P (\$/GJ)	$\dot{C}_D$ (\$/hr)	$\dot{Z}$ (\$/hr)	E (%)	Y_D(%)	r(%)	f (%)
C-100	1917.74	19.52	38.01	18.48	138.5	67.38	6.74	33.94	88.23
C-200A	5368.91	19.52	30.04	10.51	325.86	76.73	5.72	39.39	96.87
C-200B	2166.99	19.52	31.48	11.96	191.22	77.76	8.11	38.28	94.11
C-300A	3970.7	19.52	31.29	11.77	260.56	75.38	6.16	38.42	95.68
C-300B	383.59	19.52	38.96	19.43	62.13	75.95	13.94	33.38	76.17
C-400A	1709.31	19.52	33.65	14.13	153.01	75	8.22	36.72	91.55
C-400B	4577.64	19.52	29.75	10.23	307.1	77.99	6.29	39.62	96.78
TE-100	1106.11	11.81	19.52	7.71	16.83	66.82	1.5	37.69	68.58
AC-200A	686.91	19.52	19.95	0.43	3.74	97.02	0.54	49.46	89.79
AC-200B	826.84	19.52	19.95	0.43	3.74	97.02	0.45	49.46	89.79
AC-300A	269.92	19.52	19.74	0.22	1.63	98.01	0.6	49.72	88.24
AC-300B	280.85	19.52	19.76	0.24	3.74	98.01	1.31	49.7	94.03
AC-400	1807.73	19.52	20.37	0.85	6.84	95.04	0.38	48.93	88.93
E-1A	1915.12	103.31	105.68	2.38	8.13	96.79	0.42	49.43	77.38
E-1B	1423.99	103.32	105.74	2.43	5.27	96.75	0.37	49.42	68.47
E-2	2700.69	77.51	80.07	2.56	8.42	95.87	0.31	49.19	76.67
E-3	2414.93	74	78.5	4.49	4.35	93.37	0.18	48.53	49.16
T-101	1699.41	103.31	207.41	104.11	5.14	49.51	0.3	33.25	4.7

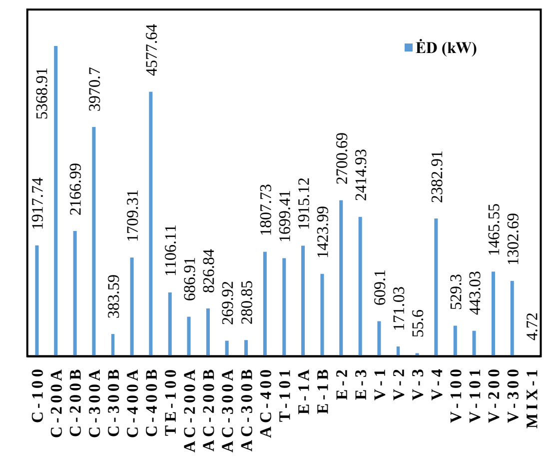

Fig. 3: Exergy destruction in each component.

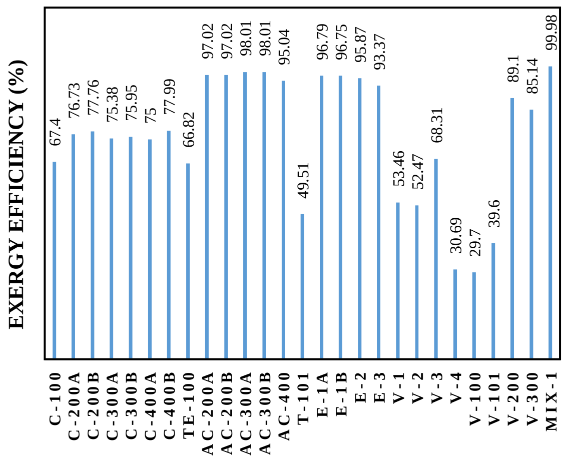

Fig. 4: Exergy efficiency in each component.

104.36\$ per gigabyte for the E-1B heat exchanger, while the maximum product cost is for the T-101 methane removal tower at 209.5 \$/GJ. The most important economic measure is the cost of the rate of degradation of the energy produced. The E-2 heat exchanger has the highest energy dissipation cost (768.90\$/GJ), and the AC-300A air conditioner has the lowest energy dissipation cost (19.35 \$/GJ) (see Figs. 5 and 6).

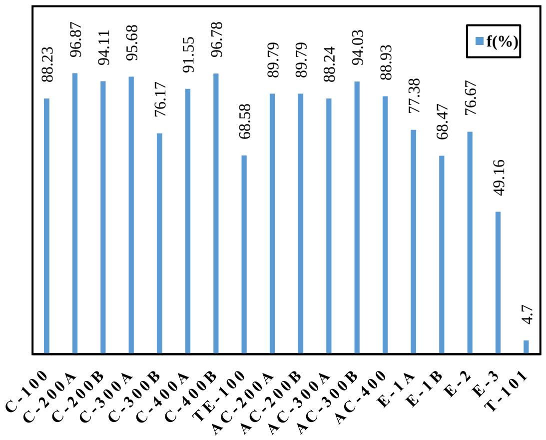

Fig. 5: Component exergoeconomic factor of each unit.

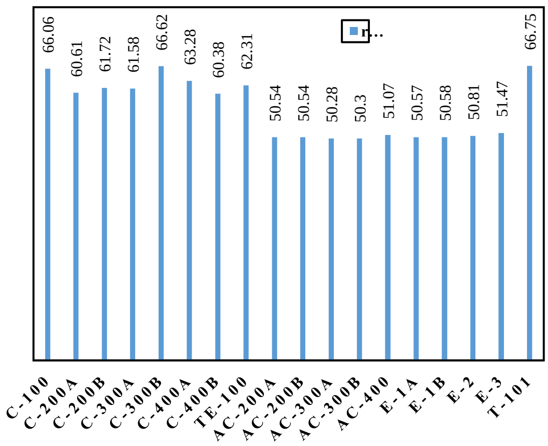

Fig. 6: Component relative cost difference of each unit.

CONCLUSIONS

This paper applies the exergy and exergoeconomic analysis for alternative operations of simultaneous production of LNG and NGL. After identifying high consumption and inefficient cases, a relationship between economic and investment costs and components with higher exergy degradation costs was proposed. External energy analysis results show that this process's external energy efficiency is about 53.82%, and its total degradation rate is equal to 42617.4 kW. The results of exergoeconomic analysis can be summarized as the cost of energy production and exergoeconomic factor as the most important elements in the cost of external energy degradation are heat exchangers due to the high value of fuel rates (defined in the exergoeconomic analysis) in these devices; the exergoeconomic factor in compressors and turbochargers is greater than the other elements, therefore, to reduce the cost of the whole system, the costs of these elements must be reduced, and the practical economic factor in heat exchangers and methane towers is negligible compared to other elements of the system, therefore, to reduce the cost of the entire system, the performance and efficiency of these elements should be maximized. According to the above conclusions, the most important elements in the cost of external energy degradation are heat exchangers. Therefore, researchers should do more about this element to improve this integral process in future studies. To reduce costs, academic and industrial experts should pay attention to reducing the costs of compressors and expansion turbos.

Acknowledgment

The authors thank the scientific support of the Amirkabir university of technology.

Received : May. 25, 2021 ; Accepted : July 19, 2021

REFERENCES

[1] Bejan A., Tsatsaronis G., Moran M., "Thermal Design and Optimization", New York, Wiley, (1996).

[2] Elliot D., Huang S., Chen J.J., Lee R.J., Yao J., Zhang Y., Benefits of Integrating NGL Extraction and LNG Liquefaction Technology, *AIChE Journal.*, (2005).

[3] Ahmadi N., Rezazadeh S., Dadvand A., Mirzaee I., Study of the Effect of Gas Channels Geometry on the Performance of Polymer Electrolyte Membrane Fuel Cell, *Periodica Polytechnica Chemical Engineering*, **62(1)**: 97-105 (2018).

[4] Ahmadi N., Rezazadeh S., Dadvand A., Mirzaee I., Modelling of Gas Transport in Proton Exchange Membrane Fuel Cells, *Proceedings of the Institution of Civil Engineers-Energy*, **170(4)**: 163-179 (2017).

[5] Ahmadi N., Kõrgesaar M. Analytical Approach to Investigate the Effect of Gas Channel Draft Angle on the Performance of PEMFC and Species Distribution, *International Journal of Heat and Mass Transfer*, **152**, (2020).

[6] Finn A.J., Developments in Natural Gas Liquefaction, *Hydrocarbon Process*, 47−59 (1999).

[7] Norouzi, N. The Pahlev Reliability Index: A Measurement for the Resilience of Power Generation Technologies Versus Climate Change, Nuclear Engineering and Technology (2020).

[8] Norouzi N., Fani M., Talebi S. Exergetic Design and Analysis of a Nuclear SMR Reactor Tetrageneration (combined water, heat, power, and chemicals) with Designed PCM energy Storage and a CO_2 Gas Turbine Inner Cycle, *Nuclear Engineering and Technology*, **53**: 677–687 (2021).

[9] Norouzi N., Hosseinpour M., Talebi S., Fani M., A 4E Analysis of Renewable Formic Acid Synthesis from the Electrochemical Reduction of Carbon Dioxide and Water: Studying Impacts of the Anolyte Material on the Performance of the Process, *Journal of Cleaner Production*, **293**, (2021).

[10] Khajehpour H., Norouzi N., Shiva N., Folourdi R. M., Bahremani E. H., Exergy Analysis and Optimization of Natural Gas Liquids Recovery Unit, *International Journal of Air-Conditioning and Refrigeration*, **29**, (2021).

[11] Norouzi N., Shiva N., Khajehpour H., Optimization of Energy Consumption in the Process of Dehumidification of Natural Gas, *Biointerface Research in Applied Chemistry*, **11**: 14634–14639 (2021).

[12] Norouzi N., Talebi S., Fani M., Khajehpour H., Exergy and Exergoeconomic Analysis of Hydrogen and Power Cogeneration Using an HTR Plant, Nuclear Engineering and Technology (2021).

[13] Norouzi N., Khajehpour H., Simulation of methane Gas Production Process from Animal Waste in a Discontinuous Bioreactor, *Biointerface Research in Applied Chemistry*, **11**: 13850–13859 (2021).

[14] Norouzi N., Talebi S., Najafi P. Thermal-Hydraulic Efficiency of a Modular Reactor Power Plant by Using the Second Law of Thermodynamic, *Annals of Nuclear Energy*, 151, (2021).

[15] Khajehpour H., Norouzi N., Fani M., An Exergetic Model for the Ambient Air Temperature Impacts on the Combined Power Plants and its Management Using the Genetic Algorithm, *International Journal of Air-Conditioning and Refrigeration*, **29**, (2021).

[16] Fani M., Norouzi N., Ramezani M., Energy, Exergy, and Exergoeconomic Analysis of Solar Thermal Power Plant Hybrid with Designed PCM Storage, *International Journal of Air-Conditioning and Refrigeration*, **28**: (2020).

[17] Gallo, W. L., Gallego, A. G., Acevedo, V. L., Dias, R., Ortiz, H. Y., Valente, B. A., Exergy Analysis of the Compression Systems and its Prime Movers for a FPSO Unit, *Journal of Natural Gas Science and Engineering*, **44**: 287–298 (2017).

[18] Ramezani F., Razmgir M., Tanha K., Nasirinezhad F., Neshasteriz A., Bahrami-Ahmadi A., Hamblin M.R., Janzadeh A., Photobiomodulation for Spinal Cord Injury: A Systematic Review and Meta-Analysis. *Physiology & Behavior*, **224**: 112977 (2020).

[19] Tashakori-Miyanroudi M., Rakhshan K., Ramez M., Asgarian S., Janzadeh A., Azizi Y., Seifalian A., Ramezani F., Conductive Carbon Nanofibers Incorporated into Collagen Bio-Scaffold Assists Myocardial Injury Repair, *International Journal of Biological Macromolecules*, **163**:1136-1146 (2020).

[20] Vahed M., Ramezani F., Tafakori V., Mirbagheri V.S., Najafi A., Ahmadian G., Molecular Dynamics Simulation and Experimental Study of the Surface-Display of SPA protein via Lpp-OmpA System for Screening of IgG, *AMB Express*, **10(1)**:1-9 (2020).

[21] Arnaiz del Pozo C., Jiménez Álvaro Á., Rodríguez Martín J., López Paniagua I. Efficiency Evaluation of Closed and Open Cycle Pure Refrigerant Cascade Natural Gas Liquefaction Process Through Exergy Analysis, *Journal of Natural Gas Science and Engineering*, **89**, (2021).

[22] Ghorbani B., Ebrahimi A., Rooholamini S., Ziabasharhagh M., Pinch and Exergy Evaluation of Kalina/Rankine/Gas/Steam Combined Power Cycles for Tri-Generation Of Power, Cooling and Hot Water Using Liquefied Natural Gas Regasification, *Energy Conversion and Management*, **223**, (2020).

[23] Zhang, S., Jiang, H., Jing, J., Qin, M., Chen, D., Chen, C., Comprehensive Comparison of Enhanced Recycle Split Vapour Processes for Ethane Recovery, *Energy Reports*, **6**: 1819–1837 (2020).

[24] Mehrpooya M., Vatani A., Moosavian S. Optimum Pressure Distribution in Design of Cryogenic NGL Recovery Processes, *Iranian Journal of Chemistry and Chemical Engineering (IJCCE)*, **31(3)**: 97-109 (2012).

[25] Ahmadi S., Nasr R. Comparative Study and Multi-Objective Optimization of Various Configurations in Natural Gas Liquefaction Process, *Iran. J. Chem. Chem. Eng. (IJCCE)*, **39(1)**: 313-336 (2020).

[26] Azari A., Shariaty-Niassar M., Alborzi M. Short-term and Medium-term Gas Demand Load Forecasting by Neural Networks, *Iranian Journal of Chemistry and Chemical Engineering (IJCCE)*, **31(4)**: 77-84 (2012). doi: 10.30492/ijcce.2012.5923

[27] Norouzi N., 4E Analysis and Design of a Combined Cycle with a Geothermal Condensing System in Iranian Moghan Diesel Power Plant, *International Journal of Air-Conditioning and Refrigeration*, **28**, (2020).

[28] Garousi Farshi L., Mahmoudi S.M.S., Rosen M.A., Exergoeconomic Comparison of Double Effect and Combined Ejector-Double Effect Absorption Refrigeration Systems, *Applied Energy*, **103**: 700–711 (2013).

[29] Ghorbani B., Salehi G.R., Amidpour M., Hamedi M.H., Exergy and Exergoeconomic Evaluation of Gas Separation Process, *Journal of Natural Gas Science and Engineering*, **9**: 86-93 (2012).

[30] Morosuk T., Tesch S., Hiemann A., Tsatsaronis G., Bin Omar N., Evaluation of the PRICO Liquefaction Process using Exergy-based Methods, *Journal of Natural Gas Science and Engineering*, 1-9 (2015).

[31] Siddiqui F.R., El-Shaarawi M.A.I., Said S.A.M, Exergoeconomic Analysis of a Solar Driven Hybrid Storage Absorption Refrigeration Cycle, *Energy Conversion and Management*, **80**: 165-172 (2014).

[32] Vatani A., Mehrpooya M., Palizdar A., Energy and Exergy Analyses of Five Conventional Liquefied Natural Gas Processes, *International Journal of Energy Research*, **38**: 1843-1863 (2014).

[33] Azizkhani A., Gandomkar A., A Novel Method for Application of Nanoparticles as Direct Asphaltene Inhibitors During Miscible CO_2 Injection, *Journal of Petroleum Science and Engineering*, 185 (2020).

[34] Pellegrini L.A., De Guido G., Valentina V., Energy and Exergy Analysis o Acid Gas Removal Processes in the LNG Production Chain, *Journal of Natural Gas Science and Engineering*, **61**: 303–319 (2019).

[35] Najibullah Khan N. B., Barifcani A., Tade M., Pareek V., A Case Study: Application of Energy And Exergy Analysis for Enhancing the Process Efficiency of a Three Stage Propane Pre-Cooling Cycle of the Cascade LNG Process, *Journal of Natural Gas Science and Engineering*, **29**: 125–133 (2016).

[36] Ghorbani B., Salehi G.R., Ghaemmaleki H., Amidpour M., Hamedi M.H., Simulation and Optimization of Refrigeration Cycle in NGL Recovery Plants with Exergy-Pinch Analysis, *Journal of Natural Gas Science and Engineering*, **7**: 35–43 (2012).

[37] Bidar B., Shahraki F. Energy and Exergo-Economic Assessments of Gas Turbine Based CHP Systems: A Case Study of SPGC Utility Plant, *Iranian Journal of Chemistry and Chemical Engineering (IJCCE)*, **37(5)**: 209-223 (2018).

[38] Noorpoor A., Mazare F., Conventional and Advanced Exergetic and Exergoeconomic Analysis Applied to an Air Preheater System for Fired Heater (Case Study: Tehran Oil Refinery Company), *Iranian Journal of Chemistry and Chemical Engineering (IJCCE)*, **37(4)**: 205-219 (2018).

[39] Khoshrou I., Jafari Nasr M., Bakhtari K. Exergy Analysis of the Optimized MSFD Type of Brackish Water Desalination Process, *Iranian Journal of Chemistry and Chemical Engineering (IJCCE)*, **36(6)**: 191-208 (2017).

[40] Norouzi N., 4E Analysis of a Fuel Cell and Gas Turbine Hybrid Energy System, *Biointerface Research in Applied Chemistry*, **11**: 7568-7579 (2021).

[41] Norouzi N., Talebi S., Fabi M., Khajehpour H., Heavy Oil Thermal Conversion and Refinement to the Green Petroleum: a Petrochemical Refinement Plant Using the Sustainable Formic Acid for the process, *Biointerface Research in Applied Chemistry*, **10**: 6088–6100 (2020).

[42] Norouzi N., Kalantari G., Talebi S., Combination of Renewable Energy in the Refinery, with Carbon Emissions Approach, *Biointerface Research in Applied Chemistry*, **10**: 5780-5786 (2020).

[43] Vessally E., Mohammadi S., Abdoli M., Hosseinian A., Ojaghloo P., Convenient and Robust Metal-Free Synthesis of Benzazole-2-Ones Through the Reaction of Aniline Derivatives and Sodium Cyanate in Aqueous Medium, *Iran. J. Chem. Chem. Eng. (IJCCE)*, **39(5)**: 11-19 (2020).

[44] Gharibzadeh F., Vessally E., Edjlali L., Es'haghi M., Mohammadi R., A DFT study on Sumanene, Corannulene and Nanosheet as the Anodes in Li−Ion Batteries, *Iran. J. Chem. Chem. Eng. (IJCCE)*, **39(6)**: 51-62 (2020).

[45] Afshar M., Khojasteh R.R., Ahmadi R., Nakhaei Moghaddam M., In Silico Adsorption of Lomustin Anticancer Drug on the Surface of Boron Nitride Nanotube, *Chem. Rev. Lett.*, **4**: 178-184 (2021).

[46] Mohammad Alipour F., Babazadeh M., Vessally E., Hosseinian, A., Delir Kheirollahi Nezhad P., A Computational Study on the Some Small Graphene-Like Nanostructures as the Anodes in Na−Ion Batteries, *Iran. J. Chem. Chem. Eng. (IJCCE)*, **40(3)**: 691-703 (2021).

[47] Hashemzadeh B., Edjlali L., Delir Kheirollahi Nezhad P., Vessally E., A DFT Studies on a Potential Anode Compound for Li-Ion Batteries: Hexa-Cata-Hexabenzocoronene Nanographen, *Chem. Rev. Lett.*, **4**: 232-238 (2021).

[48] Vessally, E., Farajzadeh, P., Najafi, E., Possible Sensing Ability of Boron Nitride Nanosheet and its Al– and Si–Doped Derivatives for Methimazole drug by Computational Study, *Iran. J. Chem. Chem. Eng. (IJCCE)*, **40(4)**: 1001-1011 (2021).

[49] Majedi S., Sreerama L., Vessally E., Behmagham F., Metal-Free Regioselective Thiocyanation of (Hetero) Aromatic C-H Bonds using Ammonium Thiocyanate: An Overview, *J. Chem. Lett.*, **1**: 25-31 (2020).

[50] Amani V., Zakeri M., Ahmadi R. Binuclear Nickel(II) Complex Containing 6-methyl-2,2'-bipyridine and Chloride Ligands: Synthesis, Characterization, Thermal Analyses, and Crystal Structure Determination, *Iran. J. Chem. Chem. Eng. (IJCCE)*, **39(2)**: 113-122 (2020).

[51] Salehi N., Vessally E., Edjlali L., Alkorta I., Eshaghi M., Nan@Tetracyanoethylene (n=1-4) Systems: Sodium salt vs Sodium electride, *Chem. Rev. Lett.*, **3**: 207-217 (2020).

[52] Soleimani-Amiri, S., Asadbeigi, N., & Badragheh, S., A Theoretical Approach to New Triplet and Quintet (nitrenoethynyl) alkylmethylenes,(nitrenoethynyl) alkylsilylenes, (nitrenoethynyl) alkylgermylenes, *Iran. J. Chem. Chem. Eng. (IJCCE)*, **39(4)**: 39-52 (2020).

[53] Sreerama, L., Vessally, E., Behmagham, F., Oxidative Lactamization of Amino Alcohols: An Overview, *J. Chem. Lett.*, **1**: 9-18 (2020).

[54] Kamel M., Mohammadifard M., Thermodynamic and Reactivity Descriptors Studies on the Interaction of Flutamide Anticancer Drug with Nucleobases: A Computational View, *Chem. Rev. Lett.*, **4**: 54-65 (2021) 54-65.

[55] Vessally E., Musavi M., Poor Heravi M.R., A Density Functional Theory Study of Adsorption Ethionamide on the Surface of the Pristine, Si and Ga and Al-Doped Graphene, *Iran. J. Chem. Chem. Eng. (IJCCE)*, **40(6)**: 1720-1736 (2021).

[56] Vakili M., Bahramzadeh V., Vakili M., A Comparative Study of SCN- Adsorption on the $Al_{12}N_{12}$, $Al_{12}P_{12}$, and Si and Ge -doped $Al_{12}N_{12}$ Nano-Cages to Remove from the Environment, *J. Chem. Lett.*, **1**: 172-178 (2020).

[57] Mosavi, M., Adsorption Behavior of Mephentermine on the Pristine and Si, Al, Ga- Doped Boron Nitride Nanosheets: DFT Studies, *J. Chem. Lett.*, **1**: 164-171 (2020).

[58] Vessally E., Siadati S.A., Hosseinian A., Edjlali L., Selective Sensing of Ozone and the Chemically Active Gaseous Species of the Troposphere by Using the C20 Fullerene and Graphene Segment, *Talanta*, **162**: 505-510 (2017).

[59] Rabipour, S., Mahmood, E. A., Afsharkhas, M., Abbasi V., A review on the cannabinoids impacts on psychiatric disorders, *Chem. Rev. Lett.* **5** 234-240(2022). 10.22034/crl.2022.349864.1175.

[60] Siadati S.A., Vessally E., Hosseinian A., Edjlali L. Possibility of Sensing, Adsorbing, and Destructing the Tabun-2D-skeletal (Tabun nerve agent) by C20 Fullerene and its Boron and Nitrogen Doped Derivatives, *Synthetic Metals*, **220**: 606-611 (2016).

[61] Rabipour S., Mahmood E.A., Afsharkha, M., Medicinal Use of Marijuana and its Impacts on Respiratory System, *J. Chem. Lett.*, **3**: 86-94 (2022).

[62] Cao Y., Soleimani-Amiri S., Ahmadi R., Issakhov A., Ebadi A.G., Vessally E., Alkoxysulfenylation of Alkenes: Development and Recent Advances, *RSC Advances*, **11**: 32513-32525 (2021).

[63] Vessally, E., Soleimani-Amiri, S., Hosseinian, A., Edjlali, L., Babazadeh, M., Chemical Fixation of CO_2 to 2-aminobenzonitriles: A Straightforward Route to Quinazoline-2, 4 (1H, 3H)-diones with Green and Sustainable Chemistry Perspectives, *J. CO_2 Util.*, **21**: 342-352 (2017).

[64] Arshadi S., Vessally E., Hosseinian A., Soleimani-Amiri S., Edjlali L. Three-Component Coupling of CO_2, Propargyl Alcohols, and Amines: an Environmentally Benign Access to Cyclic and Acyclic Carbamates (A Review), *J. CO_2 Util.*, **21**: 108-118 (2017).

[65] Kassaee M.Z., Buazar F., Soleimani-Amiri S., Triplet Germylenes with Separable Minima at ab Initio and DFT Levels, *Journal of Molecular Structure: THEOCHEM*, **866(1-3)**: 52-57 (2008).

[66] Kassaee M.Z., Aref Rad H., Soleimani Amiri S., Carbon–Nitrogen Nanorings and Nanoribbons: A Theoretical Approach for Altering the Ground States of Cyclacenes and Polyacenes, *Monatshefte für Chemie-Chemical Monthly*, **141(12)**: 1313-1319 (2010).

[67] Koohi M., Soleimani Amiri S., Haerizade B.N., Substituent Effect on Structure, Stability, and Aromaticity of Novel BnNmC20–(n+ m) Heterofullerenes, *Journal of Physical Organic Chemistry*, **30(11)**: e3682 (2017).

[68] Koohi M., Soleimani-Amiri S., Shariati M., Novel X- and Y-substituted Heterofullerenes X 4 Y 4 C 12 Developed from the Nanocage C 20, where X= B, Al, Ga, Si and Y= N, P, As, Ge: A Comparative Investigation on their Structural, Stability, and Electronic Properties at DFT, *Structural Chemistry*, **29(3)**: 909-920 (2018).

[69] Soleimani- Amiri, S. Singlet and Triplet Cyclonona-3, 5, 7- trienylidenes and Their α, ά- halogenated Derivatives at DFT, *Journal of Physical Organic Chemistry*, **33(2)**: e4018 (2020).

[70] Soleimani-Amiri S., Asadbeigi N., Badragheh S., A Theoretical Approach to New Triplet and Quintet (nitrenoethynyl) alkylmethylenes,(nitrenoethynyl) alkylsilylenes,(nitrenoethynyl) alkylgermylenes. *Iran. J. Chem. Chem. Eng. (IJCCE)*, **39(4)**: 39-52 (2020).

[71] Soleimani-Amiri, S. Identification of Structural, Spectroscopic, and Electronic Analysis of Synthesized 4-(5-Phenyl-1, 3, 4-Oxadiazol-2-Ylthio)-3-Methylbenzene-1, 2-Diol: A Theoretical Approach, *Polycyclic Aromat. Compd*, **41(3)**: 635-652 (2021).

[72] Poor Heravi M.R., Azizi B., Abdulkareem Mahmood E., Ebadi A.G., Ansari M.J., Soleimani-Amiri S., Molecular Simulation of the Paracetamol Drug Interaction with Pt-Decorated BC_3 Graphene-Like Nanosheet, *Molecular Simulation*, **48(6)**: 517-525 (2022).

[73] Ghazvini M., Sheikholeslami-Farahani F., Soleimani-Amiri S., Salimifard M., Rostamian R., Green Synthesis of Pyrido [2, 1-a] isoquinolines and Pyrido [1, 2-a] Quinolines by Using ZnO Nanoparticles, *Synlett*, **29(04)**: 493-496 (2018).

[74] Soleimani- Amiri S., Shafaei F., Varasteh Moradi A., Gholami- Orimi F., Rostami Z., A Novel Synthesis and Antioxidant Evaluation of Functionalized [1, 3]-Oxazoles Using Fe_3O_4- Magnetic Nanoparticles, *Journal of Heterocyclic Chemistry*, **56(10)**: 2744-2752 (2019).

[75] Soleimani Amiri S., Green Production and Antioxidant Activity Study of New Pyrrolo [2, 1- a] Isoquinolines, *J. Heterocyclic Chem.*, **57(11)**: 4057-4069 (2020).

[76] Samiei Z., Soleimani-Amiri S., Azizi Z., Fe_3O_4@ C@ OSO_3H as an Efficient, Recyclable Magnetic Nanocatalyst in Pechmann Condensation: Green Synthesis, Characterization, and Theoretical Study, *Molecular Diversity*, **25(1)**: 67-86 (2021).

[77] Taheri Hatkehlouei S.F., Mirza B., Soleimani-Amiri S., Solvent-free One-Pot Synthesis of Diverse Dihydropyrimidinones/Tetrahydropyrimidinones Using Biginelli Reaction Catalyzed by Fe3O4@ C@ OSO3H, *Polycyclic Aromat. Compd*, **42(4)**: 1341-1357 (2022).

[78] Amiri S.S., Ghazvini M., Khandan S., Afrashteh S., KF/Clinoptilolite@ MWCNTs Nanocomposites Promoted a Novel Four-Component Reaction of Isocyanides for the Green Synthesis of Pyrimidoisoquinolines in Water, *Polycyclic Aromat. Compd.*, **42**: 1-16 (2021).

[79] Zarei F., Soleimani-Amiri S., Azizi Z., Heterogeneously Catalyzed Pechmann Condensation Employing the HFe (SO_4) 2.4 H_2O-Chitosan Nano-Composite: Ultrasound-Accelerated Green Synthesis of Coumarins, *Polycyclic Aromat. Compd.*,: 1-18 (2021).

[80] Feizpour Bonab M., Soleimani-Amiri S., Mirza B., Fe3O4@ C@ PrS-SO3H: A Novel Efficient Magnetically Recoverable Heterogeneous Catalyst in the Ultrasound-Assisted Synthesis of Coumarin Derivatives, *Polycyclic Aromat. Compd*, 1-16 (2022).

[81] Soleimani-Amiri, S., Hossaini, Z., Azizi, Z., Synthesis and Investigation of Biological Activity of New Oxazinoazepines: Application of Fe_3O_4/CuO/ZnO@ MWCNT Magnetic Nanocomposite in Reduction of 4-Nitrophenol in Water, *Polycyclic Aromat. Compd.*, 1-22 (2022).

[82] Khoshtarkib, Z., Ebadi, A., Alizadeh, R., Ahmadi, R., Amani, V., Dichloridobis (phenanthridine-κN) zinc (II). *Acta Crystallog.* E: 65(7): m739-m740 (2009).

[83] Salehi N., Chemical composition of the Essential oil from Aerial parts of Achillea filipendulina Lam. from Iran, *J. Chem. Lett.*, **1**: 160-163 (2020).

[84] Amani V., Ahmadi R., Naseh M., Ebadi A. Synthesis, Spectroscopic Characterization, Crystal Structure and Thermal Analyses of Two Zinc (II) Complexes with Methanolysis of 2-Pyridinecarbonitrile as a Chelating Ligand, *JICS*, **14(3)**: 635-642 (2017).

[85] Iji M., Dass P.M., Shalbugau K.W., Penuel B.L., Synthesis and Characterization of Heterogeneous Catalysts from Magnetic Sand and Kaolin, *Journal of Chemistry Letters*, **1(3)**: 139-142 (2020)

[86] Ahmadi R., Khalighi A., Kalateh K., Amani V., Khavasi H. R. catena-Poly [[(5, 5′-dimethyl-2, 2′-bipyridine-κ2N, N′) cadmium (II)]-di-μ-chlorido]. *Acta Crystallog*. E: 64(10): m1233-m1233 (2008).

[87] Benhachem F.Z., Harrache D., Evaluation of Physico-Chemical Quality And Metallic Contamination Level of Epikarstic Seepage Waters in Forest Zone, *J. Chem. Lett.*, **1**: 59-62 (2020).

[88] Soleimani- Amiri S., Arabkhazaeli M., Hossaini Z., Afrashteh S., Eslami A. A. Synthesis of Chromene Derivatives via Three- Component Reaction of 4-hydroxycumarin Catalyzed by Magnetic Fe_3O_4 Nanoparticles in Water, *Journal of Heterocyclic Chemistry*, **55(1)**: 209-213 (2018).

[89] Soleimani- Amiri S., Hossaini Z., Arabkhazaeli M., Karami H., Afshari Sharif Abad S., Green synthesis of Pyrimido- isoquinolines and Pyrimido- Quinoline Using ZnO Nanorods as an Efficient Catalyst: Study Of Antioxidant Activity, *Journal of the Chinese Chemical Society*, **66(4)**: 438-445 (2019).

[90] Norouzi N. Dynamic Modeling of the Effect of Vehicle Hybridization Policy on Carbon Emission and Energy Consumption, *J. Chem. Lett*, **3**: 99-106 (2022).

[91] Soleimani- Amiri S., Hossaini Z., Azizi Z., Synthesis and Investigation of Antioxidant and Antimicrobial Activity of New Pyrazinopyrroloazepine Derivatives Using Fe_3O_4/CuO/ZnO@MWCNT MNCs as Organometallic Nanocatalyst by new MCRs, *Appl. Organomet. Chem.*, **36(4)**: e6573 (2022).

[92] Karbakhshzadeh A., Majedi S., Abbasi V., Computational Investigation on Interaction Between Graphene Nanostructure BC_3 and Rimantadine Drug, *J. Chem. Lett.*, **3**: 108-113 (2022).

[93] Norouzi N., Ebadi A. G., Bozorgian A., Vessally E., Hoseyni S. J., Energy and Exergy Analysis of Internal Combustion Engine Performance of Spark Ignition for Gasoline, Methane, and Hydrogen Fuels, *Iran. J. Chem. Chem. Eng. (IJCCE).*, **40(6)**: 1909-1930 (2021).

[94] Rabipour S., Mahmood E. A., Afsharkhas M., Abbasi V., Cannabinoids Impact on Cognition: A Review from the Neurobiological Perspective, *Chem. Rev. Lett.*, **6**: 7-14 (2023).

[95] Norouzi N., Ebadi A. G., Bozorgian A., Hoseyni S. J., Vessally E., Cogeneration System of Power, Cooling, and Hydrogen from Geothermal Energy: An Exergy Approach, *Iran. J. Chem. Chem. Eng. (IJCCE)*, **41(2)**: 706-721 (2022).

[96] Silas K., Musa Y.P., Habiba M.D., Effective Application of Jatropha Curcas Husk Activated $ZnCl_2$, *Chem. Rev. Lett.*, **5**: 153-160 (2022).

[97] Khezri A., Edjlali L., Eshaghi M., Vardini M.T., Basharnavaz H., A novel [3-(4-methoxyphenyl)isoxazole-5-yl]-methanol Compound: Synthesis, *Chem. Rev. Lett.*, **5**: 113-118 (2022).

[98] Hoseyni S.J., Manoochehri M., Asli M.D., Synthesis and Crystal Structure of Dibromido{[(2-Pyridyl) methyl](p-ethylphenyl)amine}Zinc, *Chem. Rev. Lett.*, **5**: 99-105 (2022).

[99] Kadhim M.M., Mahmood E.A., Abbasi V., Poor Heravi M.R., Habibzadeh S., Mohammadi-Aghdam S., Soleimani-Amiri S., Theoretical Investigation of the Titanium—Nitrogen Heterofullerenes Evolved from the Smallest Fullerene, *J. Mol. Graph. Model.*, (2022).

[100] Porgar S., Rahmanian N., Phase equilibrium for hydrate formation in the Methane and Ethane System and Effect of Inhibitors, *Chem. Rev. Lett.*, **5**: 2-11 (2022).

[101] Kadhim M.M., Mahmood E.A., Abbasi V., Poor Heravi M.R., Habibzadeh S., Mohammadi-Aghdam S., Shoaei S.M., Theoretical Investigation of the Titanium—Nitrogen Heterofullerenes Evolved from the Smallest Fullerene, *J. Mol. Graph. Model.*, **117**: 108269 (2022).

[102] Avşar C., Tümük D., Ertunç S., Gezerman A.O., A Review on Ammono-Carbonation Reactions: Focusing on the Merseburg Process, *Chem. Rev. Lett.*, **5**: 83-91 (2022).

[103] Rabipour S., Mahmood E., Ebadi A., Bozorgian A., Vessally E., Asadi Z., Afsharkhas M., A Systematic Review of Therapeutic Potential of Illicit Drugs: A Narrative Overview of How Cannabinoids and Psychedelics Can be Used in Medicine, *Iran. J. Chem. Chem. Eng. (IJCCE)*, **41(3)**: 722-752 (2022).